Mesoporous Ca-Mn-O as Efficient Scavenger toward Organic Pollutants and Heavy Metals: Ion Exchange Provoking Ultrafast Fenton-like Reaction based on the Synergy of Alkaline Earth/Transition Metals

Yali Weng[a,b], Zhenzhang Weng[a,b], Zhiyu Liang[a,b], Haixia Lyu[a,b], Zanyong Zhuang[a,b]*, Yan Yu[a,b]*

[a] College of Materials Science and Engineering, Fuzhou University, New Campus, Minhou, Fujian Province 350108, China

[b] Key Laboratory of Eco-materials Advanced Technology (Fuzhou University), Fujian Province University, Fujian Province 350108, China

*Corresponding author. Fax: +86 591 22866534;

E-mail address: zyzhuang@fzu.edu.cn, yuyan_1972@126.com

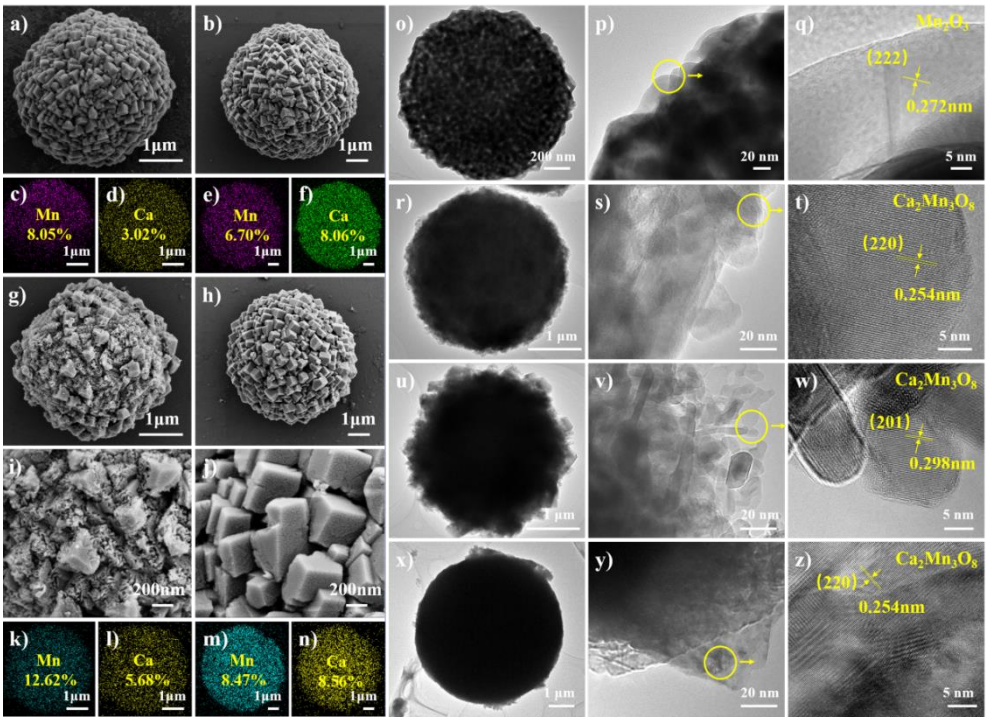

Figure S1. SEM images of (a) $CaMn_2(CO_3)_3$, (b) $CaMn(CO_3)_2$, (g) $CaMn_2$ and (h) CaMn; corresponding elemental mapping of Mn and Ca on above microspheres (c-f) and (k-n); Low- and high-magnification TEM images of (o-q) Mn_2O_3, (r–t) $CaMn_3$, (u–w) $CaMn_2$, (x–z) CaMn.

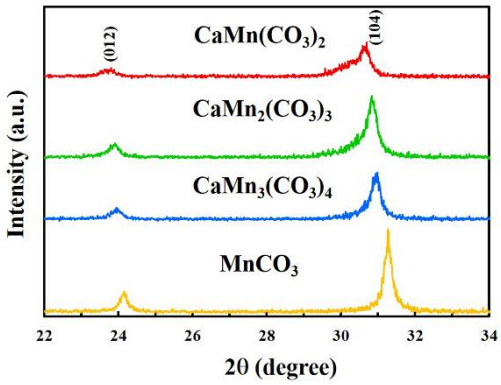

Figure S2. XRD enlarge patterns of the carbonates spheres with 2θ ranging from 22° to 34°.

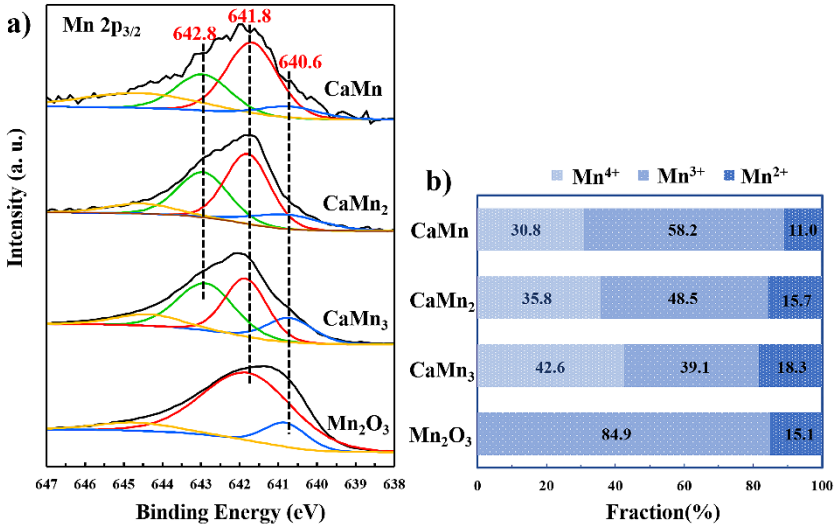

Figure S3. (a) X-ray photoelectron spectroscopy (XPS) survey spectra of Mn $2p_{3/2}$; (b) Fractions of Mn species in the unreacted samples of Mn_2O_3, $CaMn_3$, $CaMn_2$ and CaMn.

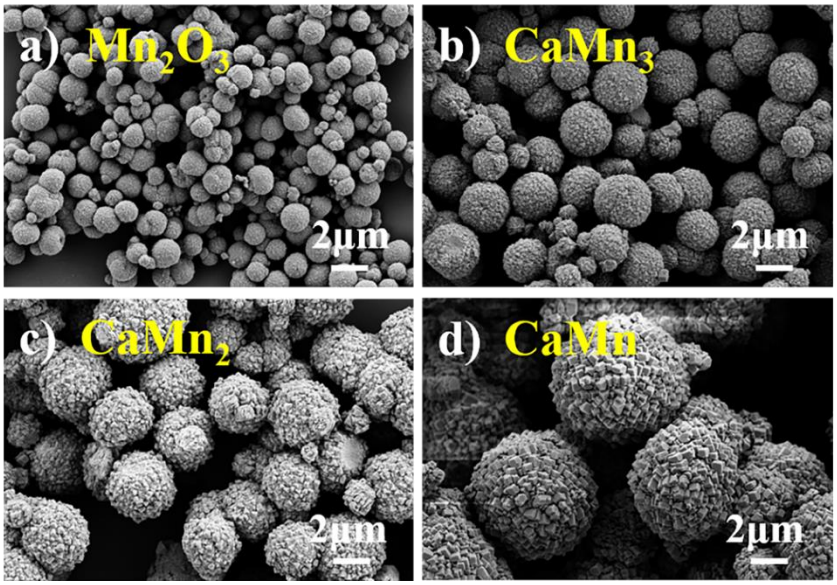

Figure S4. SEM images of (a) Mn_2O_3, (b) $CaMn_3$, (c) $CaMn_2$, and (d) CaMn.

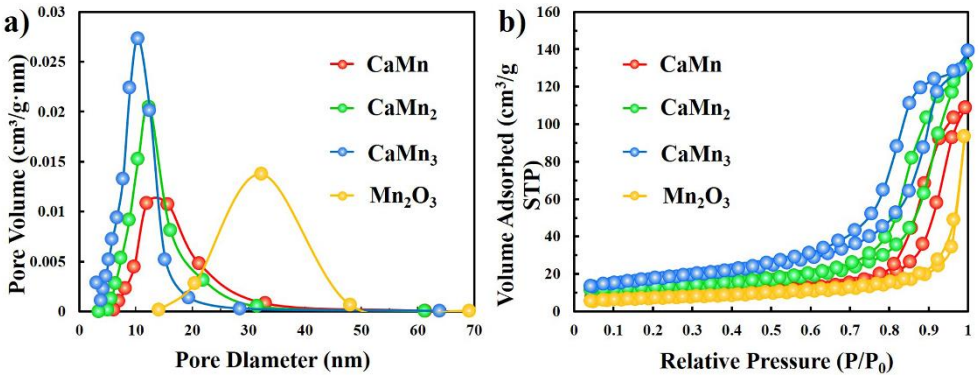

Figure S5. Structural characterization of Ca-Mn mixed oxides with different Ca/Mn molar ratios including pure Mn_2O_3: (a) BJH adsorption pore size distributions; (b) nitrogen sorption isotherms.

Table S1. Structural characteristics of Mn_2O_3 and $CaMn_x$.

	BET surface area (m^2/g)	Pore volume (cm^3/g)	Pore size (nm)
CaMn	27.0	0.169	17.8
$CaMn_2$	45.9	0.214	14.6
$CaMn_3$	59.6	0.201	10.4
Mn_2O_3	19.6	0.246	30.8

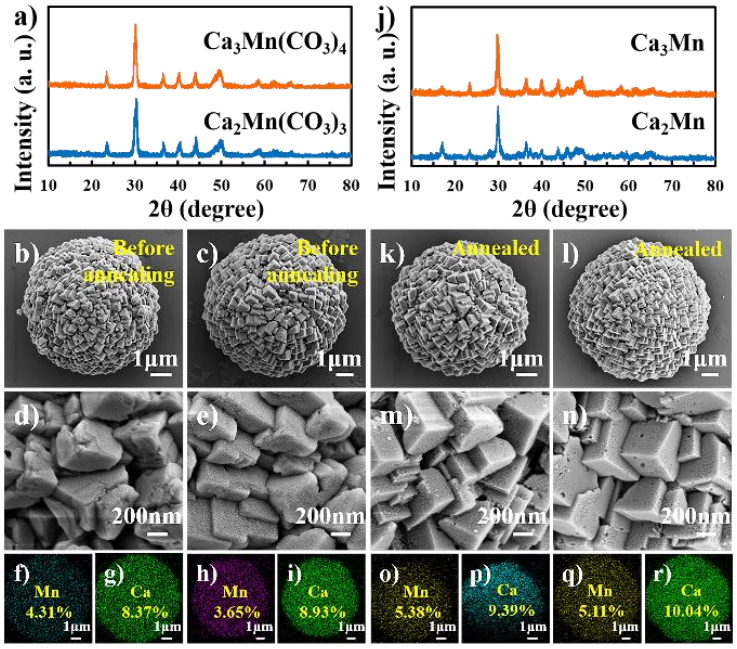

Figure S6. XRD patterns of (a) carbonates spheres and (j) annealed samples; SEM images of (b, d) $Ca_2Mn(CO_3)_3$, (c, e) $Ca_3Mn(CO_3)_4$, (k, m) Ca_2Mn and (l, n) Ca_3Mn. (f-i) and (o-r) show elemental mapping of Mn or Ca on above samples.

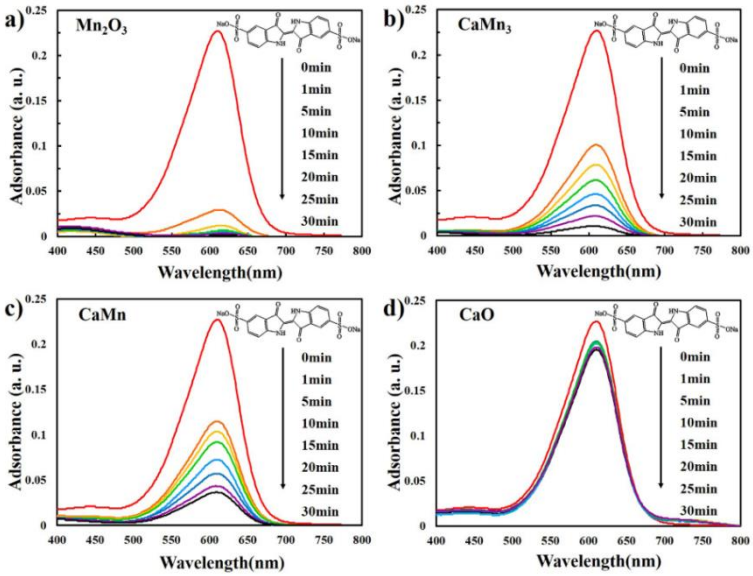

Figure S7. UV-Vis absorption spectra of indigo carmine solution in the presence of (a) Mn_2O_3, (b) $CaMn_3$, (c) CaMn and (d) CaO (V = 50 mL, pH = 6.3 ± 0.1, [indigo carmine] = 10 mg L^{-1}, adsorbent materials = 0.5 g L^{-1}).

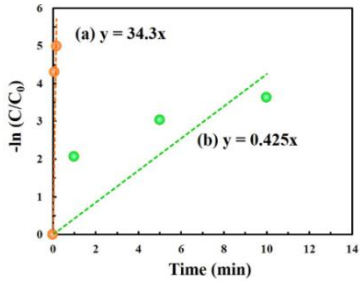

Figure S8. The kinetic fitting of indigo carmine degradation: (a) $CaMn_2$ in presence of metal ions and (b) Mn_2O_3 in pure indigo carmine solution. Actually, the line b did not follow the linear fitting between $\ln(C/C_0)$ and time, because it involves of adsorption process rather than oxidant reaction. To compared with line a, the line a was still roughly fitted using the same model.

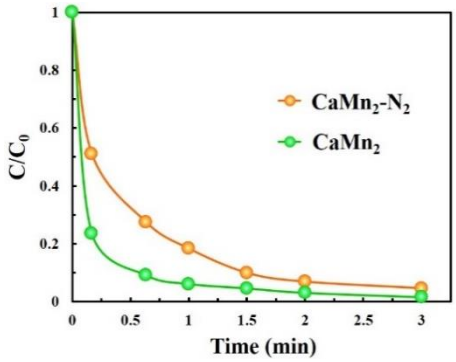

Figure S9. Removal of indigo carmine by $CaMn_2$ under the air or in the presence of N_2 (V =50 mL, pH = 5.8 ± 0.1, [indigo carmine] = [metal ions] = 20 mg L^{-1}, [$CaMn_2$] = 0.5 g L^{-1}). It should be noted that, in our experiment, we cannot exclude the O_2 completely, since there could be part of O_2 dissolved during the extraction and centrifugation of aliquot sample.

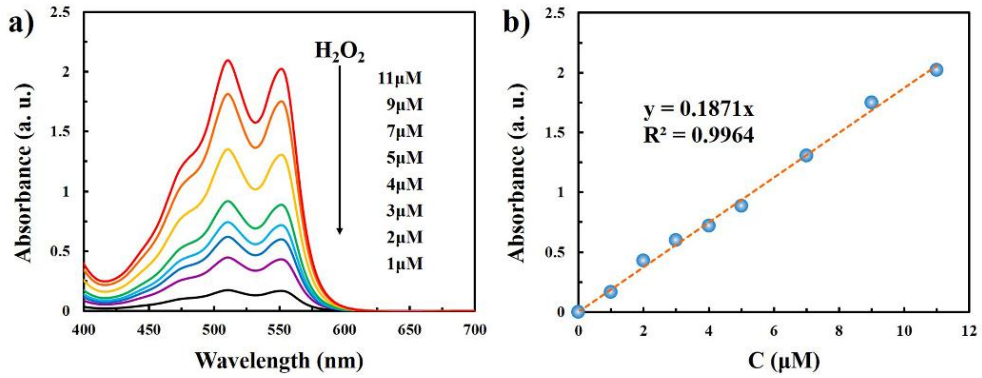

Figure S10. (a) UV-vis spectra and (b) the standard curve of absorbance vs H_2O_2 concentration (1 to 11 μM) recorded at 551 nm. The curves were obtained by the addition of DPD (50 μL) and POD (50 μL) to the sampled aliquots and measuring the UV-vis spectra of the resulting solution.

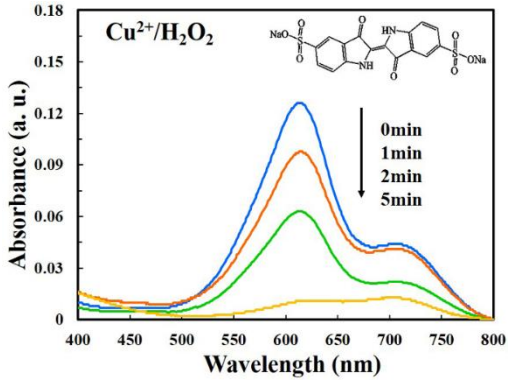

Figure S11. UV-vis absorption spectra of 10 mg L^{-1} indigo carmine solution after treatment by homogeneous Cu^{2+}/H_2O_2 (10 mg L^{-1} Cu^{2+}/10 μM H_2O_2) catalyst.

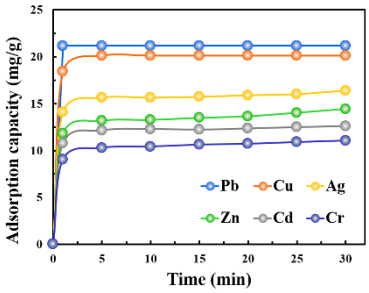

Figure S12. The adsorption isotherms of Pb^{2+}, Cu^{2+}, Cd^{2+}, Ag^{+}, Zn^{2+} and Cr^{3+} by $CaMn_2$. V = 50 mL, pH=5.8 ± 0.1, [indigo carmine] = [congo red] = [orange G] = 10 mg L^{-1}, [metal ions] =10 mg L^{-1}, [$CaMn_2$] = 0.5 mg L^{-1}.

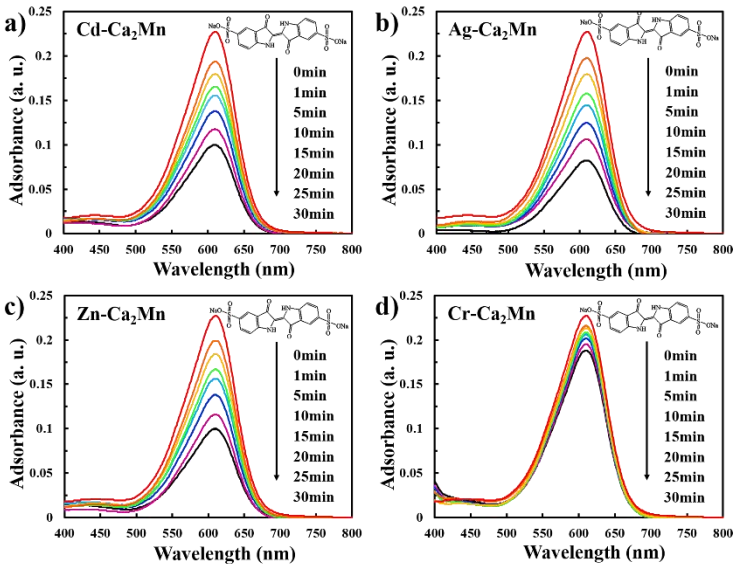

Figure S13. The UV-vis absorption spectra of wastewater samples containing indigo carmine after treated by (a) Cd-$CaMn_2$, (b) Ag-$CaMn_2$, (c) Zn-$CaMn_2$ and (d) Cr-$CaMn_2$ (V=50 mL, pH = 6.3 ± 0.1, [indigo carmine]=10 mg L^{-1}, [Cd-$CaMn_2$] =[Ag-$CaMn_2$]=[Zn-$CaMn_2$] =[Cr-$CaMn_2$]=0.5 g L^{-1}).

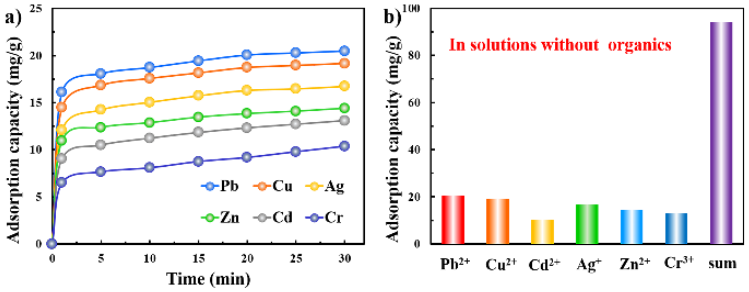

Figure S14. (a) The adsorption isotherms of Pb^{2+}, Cu^{2+}, Cd^{2+}, Ag^{+}, Zn^{2+} and Cr^{3+} by $CaMn_2$ in the organic-free solution; (b) the adsorption capacity of (a) with coexisting Pb^{2+}, Cu^{2+}, Cd^{2+}, Ag^{+}, Zn^{2+}, Cr^{3+} and their sum by $CaMn_2$.

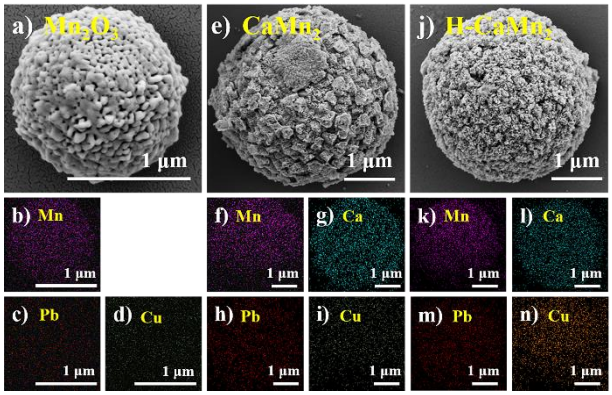

Figure S15. SEM images and the corresponding elemental mapping of samples after four recycling tests: (a-d) Mn_2O_3, (e-i) $CaMn_2$ and (j-n) H-$CaMn_2$.

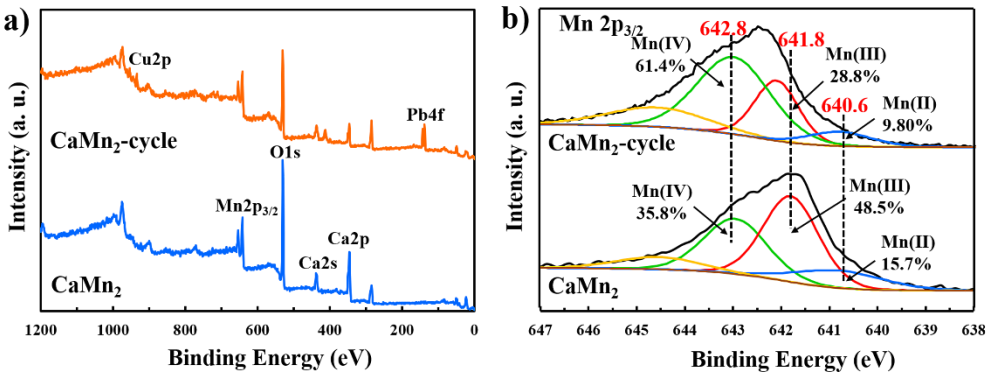

Figure S16. (a) XPS survey spectra of $CaMn_2$ and $CaMn_2$-cycle; (b) Corresponding high-resolution XPS spectra Mn $2p_{3/2}$ of the $CaMn_2$ and $CaMn_2$-cycle, respectively.

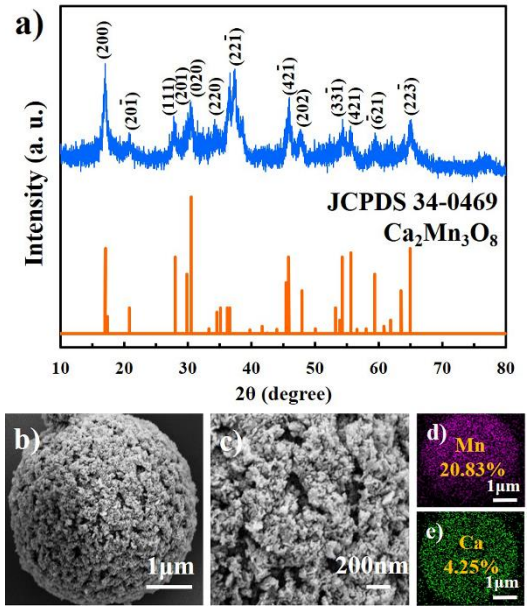

Figure S17. (a) XRD patterns of H-$CaMn_2$ ($CaMn_2$ was etched by 0.01M HCl and rinsed with distilled water several times to remove the impurities; (b-c) SEM images of H-$CaMn_2$; (d-c) corresponding elemental mapping of Mn or Ca on the sample H-$CaMn_2$.